J Sci Comput (2010) 42: 291–317
DOI 10.1007/s10915-009-9325-x

A Collocation Method with Exact Imposition of Mixed Boundary Conditions

Zhong-Qing Wang · Li-Lian Wang

Received: 3 May 2009 / Revised: 3 September 2009 / Accepted: 8 September 2009 /
Published online: 22 September 2009

Abstract In this paper, we propose a natural collocation method with exact imposition of mixed boundary conditions based on a generalized Gauss-Lobatto-Legendre-Birhoff quadrature rule that builds in the underlying boundary data. We provide a direct construction of the quadrature rule, and show that the collocation method can be implemented as efficiently as the usual collocation scheme for PDEs with Dirichlet boundary conditions. We apply the collocation method to some model PDEs and the time-harmonic Helmholtz equation, and demonstrate its spectral accuracy and efficiency by various numerical examples.

Keywords Quadrature formulae · Mixed boundary conditions · Collocation methods · Spectral accuracy

The work of the first author is supported in part by National Basic Research Project of China N.2005CB321701, NSF of China, N.10771142, Science and Technology Commission of Shanghai Municipality Grant, N.075105118, Shuguang Project of Shanghai Education Commission, N.08SG45, Shanghai Leading Academic Discipline Project N.S30405 and The Fund for E-institute of Shanghai Universities N.E03004.
The work of the second author is partially supported by AcRF Tier 1 Grant RG58/08, Singapore MOE Grant # T207B2202, and Singapore # NRF2007IDM-IDM002-010.

Z.-Q. Wang
Department of Mathematics, Shanghai Normal University, Shanghai 200234, People's Republic of China

Z.-Q. Wang
Scientific Computing Key Laboratory, Shanghai Universities, Shanghai, People's Republic of China

Z.-Q. Wang
Division of Computational Science of E-institute, Shanghai Universities, Shanghai, People's Republic of China

L.-L. Wang (✉)
Division of Mathematical Sciences, School of Physical and Mathematical Sciences, Nanyang Technological University, Singapore 637371, Singapore
e-mail: LiLian@ntu.edu.sg

1 Introduction

In the past several decades, spectral method has become increasingly popular in scientific computing and engineering applications (cf. [3, 4, 6, 7, 16] and the references therein). Among several spectral approaches, the collocation method is known to be well-suited for nonlinear problems partially owing to its implementation in physical space. Moreover, it oftentimes leads to simple mass matrices, and therefore exhibits some remarkable advantages in the context of lumped mass techniques and explicit time-discretizations of PDEs [11, 25]. In a collocation method, the choice of collocation points is crucial for accuracy, stability and ease of treating boundary conditions [13, 19]. It is known that the collocation points are usually chosen as the quadrature nodes of certain Gauss-type quadrature rule. In particular, the collocation methods based on Gauss-Lobatto and Gauss-Radau points have been widely used in solving first- and second-order equations, where the endpoints (i.e., the boundary data) are built in the quadrature formulas. However, as pointed in [19], the usual Gauss-Lobatto collocation method may induce numerical instability, when it applies to third-order equations. To fix the problem, it is advisable to choose collocation points associated with some generalized Gauss-quadratures. More precisely, given a $(R+L)$th order differential equation with Dirichlet boundary conditions:

$$u^{(l)}(-1)=\alpha_l, \quad 0\le l\le L-1; \qquad u^{(r)}(1)=\beta_r, \quad 0\le r\le R-1, \tag{1.1}$$

it is natural to associate the collocation method with the generalized Gauss-quadrature (see, e.g., [3, 13]):

$$\int_{-1}^{1} u(x)dx \sim \sum_{l=0}^{L-1} u^{(l)}(-1)\omega_l^- + \sum_{j=1}^{N} u(x_j)\omega_j + \sum_{r=0}^{R-1} u^{(r)}(1)\omega_r^+, \tag{1.2}$$

where the interior nodes $\{x_j\}_{j=1}^N$ are chosen as the zeros of certain Jacobi polynomial, so that the resulting rule enjoys the maximum degree of precision. Some polynomial interpolation approximation results in Sobolev spaces were derived in [3, 27], and the collocation method based on the rule (1.2) with $R=1$ and $L=2$ was analyzed for third-order equations in [18].

The purpose of this paper is to construct collocation methods for second-order boundary value problems with general mixed boundary conditions:

$$\mathcal{B}_-u := a_-u'(-1)+b_-u(-1)=\alpha_-; \qquad \mathcal{B}_+u := a_+u'(1)+b_+u(1)=\alpha_+. \tag{1.3}$$

As the starting point, we build the boundary data in the quadrature rule of the form

$$\int_{-1}^{1} u(x)dx \sim \omega_-\mathcal{B}_-u + \sum_{j=1}^{N} u(x_j)\omega_j + \omega_+\mathcal{B}_+u, \tag{1.4}$$

which has the maximum degree of precision $2N+1$, and whose interior nodes $\{x_j\}_{j=1}^N$ must lie in $(-1,1)$. This rule is referred to as the Legendre-Gauss-Lobatto-Birkhoff quadrature. In fact, Ezzirani and Guessab [10] discussed some Birkhoff-type quadratures (cf. [9, 15, 28]) with more general mixed boundary functionals, and some assumptions on the boundary functionals were assumed to guarantee the existence of the rules. In principle, we may apply the general results in [10] to show the existence of (1.4), but the assumption leads to severe constraints on the constants $\alpha_\pm$ and $\beta_\pm$. To fix the problem, we take a direct approach to construct (1.4). Notice that the boundary condition (1.3) must fall into one of the four cases:

(i) $u(-1)=\alpha_-$ and $u(1)=\alpha_+$;
(ii) $u'(-1)=\alpha_-$ and $u'(1)=\alpha_+$;
(iii) $u(-1)=\alpha_-$ and $u'(1)+\mu u(1)=\alpha_+$ (the case with mixed data at -1 can be treated with a change of variable $x\to -x$);
(iv) $u'(-1)+au(-1)=\alpha_-$ and $u'(1)+bu(1)=\alpha_+$ (with $a^2+b^2\neq 0$).

The paper [10] gave much attention to the quadrature formula for (ii) (i.e., (1.4) with $a_\pm=1$ and $b_\pm=0$) and applied it to lumped mass collocation approximations of pure Neumann problems. A rigorous analysis of the polynomial interpolation errors in Sobolev spaces was carried out in [26].

In this paper, we focus on the case (iii). We start with the existence and a direct construction of the quadrature rule, and then develop the collocation methods for some model linear problems and the time-harmonic Helmholtz equation. We show that the quadrature rule exists for almost all real constant μ, and the resultant collocation methods can be naturally implemented as efficiently as the usual Gauss-Lobatto collocation schemes for problems with Dirichlet data. Consequently, it is also natural to design the lumped mass spectral approximations to mixed boundary conditions. Moreover, such an approach provides a stable approximation to mixed boundary condition problems, while the standard collocation method might suffer from numerical instability. On the other hand, the finite difference preconditioning can be applied to obtain a well-behaved collocation system. It should be pointed out that the argument and idea can be extended to the case (iv) straightforwardly but with possible complications from dealing with two parameters.

The rest of the paper is organized as follows. We construct the quadrature formula that builds in the mixed data (iii), and introduce an algorithm for the evaluation of the nodes and weights in Sect. 2. We implement in Sect. 3 the collocation methods for one- and two-dimensional problems, and apply the methods for solving the time-harmonic Helmholtz equation with high wave number in Sect. 4. We end this section with some notations to be used throughout the paper.

① Let $\omega^{(\alpha,\beta)}(x)=(1-x)^\alpha(1+x)^\beta,\ x\in(-1,1)$ with $\alpha,\ \beta>-1$ be the Jacobi weight function.
② Let $\mathbb{N}$ be the set of all non-negative integers. For any $N\in\mathbb{N}$, let $\mathbb{P}_N$ be the set of all algebraic polynomials of degree at most N.
③ For simplicity, we sometimes denote $\partial_x^l v=\frac{d^l v}{dx^l}=v^{(l)}$, for any integer $l\geq 1$.

2 Quadrature Formula

We are interested in the quadrature rule associated with the boundary conditions (iii):

$$\int_{-1}^{1}\phi(x)dx=\phi(-1)\omega_0+\sum_{j=1}^{N}\phi(x_j)\omega_j+\big(\phi'(1)+\mu\phi(1)\big)\omega_{N+1},\qquad \forall\phi\in\mathbb{P}_{2N+1},\tag{2.1}$$

where the nodes $\{x_j\}_{j=1}^N$ lie in $(-1,1)$. We start with the construction of such a rule, followed by the numerical evaluation of the nodes and weights.

2.1 Construction

Let $\pi_n^{(2,1)}(x)$ be the monic Jacobi polynomial of degree n as defined in (A.8). As to be shown in Theorem 2.1, the interior nodes $\{x_j\}_{j=1}^N$ are zeros of the quasi-orthogonal polynomial:

$$Q_N(x)=\pi_N^{(2,1)}(x)+\rho\pi_{N-1}^{(2,1)}(x),\tag{2.2}$$

where the constant $\rho := \rho(N, \mu)$ is chosen such that

(a) all N zeros of Q_N must lie in $(-1, 1)$;
(b) the following important relation for the existence of (2.1) holds:

$$\int_{-1}^{1} \Psi_N(x)dx = 0, \tag{2.3}$$

where

$$\Psi_N(x) = (x+1)\big[\big((2\mu+1)Q_N(1) + 2Q_N'(1)\big)x - (2\mu+3)Q_N(1) - 2Q_N'(1)\big]Q_N(x). \tag{2.4}$$

As a preparation for the proof of the main result, we first seek the explicit expression of ρ in (2.2). To meet the requirement (a), we deduce from Theorem 3.3.4 of [24] that Q_N *has exactly* N *distinct zeros, and all of them lie in* $(-1, 1)$ *if and only if*

$$\rho_{\min} := -\frac{(N+2)(N+3)}{(N+1)(2N+3)} = -\frac{\pi_N^{(2,1)}(1)}{\pi_{N-1}^{(2,1)}(1)} < \rho < -\frac{\pi_N^{(2,1)}(-1)}{\pi_{N-1}^{(2,1)}(-1)} = \frac{N+3}{2N+3} := \rho_{\max}, \tag{2.5}$$

where we used (A.5), (A.6) and (A.8) to work out the constants.

We next examine the condition (b). Using (A.6)–(A.8) and the formula (see, e.g., [1]):

$$\int_{-1}^{1} J_k^{(2,1)}(x)\omega^{(\alpha,1)}(x)dx = \frac{2^{\alpha+2}(k+1)\Gamma(\alpha+1)\Gamma(k-\alpha+2)}{\Gamma(2-\alpha)\Gamma(k+\alpha+3)}, \quad -1<\alpha<2, \tag{2.6}$$

we find that (2.3)–(2.4) is reduced to

$$g(\rho) := A\rho^2 + B\rho + C = 0, \tag{2.7}$$

where

$$A = \frac{2\mu}{N} + \frac{4}{3}(N+2),$$
$$B = \frac{4\mu(N^2+3N+3)}{N(N+1)(2N+3)} + \frac{(N+2)(\frac{2}{3}N^2+2N+3)}{N(2N+3)} + \frac{(N+3)(2N^2+6N+5)}{(N+1)(2N+3)},$$
$$C = \frac{2\mu(N+2)(N+3)}{(N+1)(2N+3)^2} + \frac{4(N+2)(N+3)^2}{3(2N+3)^2}.$$

We now process with two separated cases to determine ρ.

(i) $A = 0$, i.e., $\mu = -\frac{2}{3}N(N+2)$. In this case, the unique root of (2.7) is

$$\rho = -\frac{2N(N+2)(N+3)}{(2N+3)(2N^2+4N+3)}. \tag{2.8}$$

It is clear that $\rho \in (\rho_{\min}, \rho_{\max})$, so this ρ meets our need.

(ii) $A \neq 0$. One verifies that for any real number μ and integer N, $B^2 - 4AC > 0$. Indeed, a direct calculation shows that

$$B^2 - 4AC = \frac{4(A_1\mu^2 + B_1\mu + C_1)}{3N^2(N+1)^2},$$

where $A_1 = 12$, $B_1 = 12N^2 + 36N + 12$ and $C_1 = 4N^4 + 24N^3 + 44N^2 + 24N + 3$. On the other hand,

$$B_1^2 - 4A_1C_1 = -48N^4 - 288N^3 - 528N^2 - 288N < 0.$$

Hence, $A_1\mu^2 + B_1\mu + C_1 > 0$, and $B^2 - 4AC > 0$. Denote the two (real) roots of (2.7) by

$$\rho_1 = \frac{-B + \sqrt{B^2 - 4AC}}{2A}, \qquad \rho_2 = \frac{-B - \sqrt{B^2 - 4AC}}{2A}. \tag{2.9}$$

It is clear that if $g(\rho_{\min})g(\rho_{\max}) < 0$, i.e.,

$$\mu > \mu_0 := -\frac{2}{3}N^2 - 2N - \frac{1}{3}, \tag{2.10}$$

there exists exactly one root of (2.7) in $(\rho_{\min}, \rho_{\max})$. In fact, we are able to find that $\rho = \rho_1 \in (\rho_{\min}, \rho_{\max})$. Indeed, a direct calculation leads to

$$B > B|_{\mu=\mu_0} = \frac{2}{N(N+1)(2N+3)} > 0,$$
$$C > C|_{\mu=\mu_0} = \frac{2(N+2)(N+3)(2N+5)}{3(N+1)(2N+3)^2} > 0.$$

Hence, if $A > 0$, then $\rho_2 < \rho_1 < 0$, and therefore ρ_1 belongs to $(\rho_{\min}, \rho_{\max})$. On the other hand, if $A < 0$, then $\rho_1 < 0$, $\rho_2 > 0$ and $|\rho_1| < |\rho_2|$, which, together with the fact: $\rho_{\min} < 0$, $\rho_{\max} > 0$ and $|\rho_{\min}| > |\rho_{\max}|$, implies that $\rho = \rho_1 \in (\rho_{\min}, \rho_{\max})$.

It remains to consider the case: $g(\rho_{\min})g(\rho_{\max}) \ge 0$, i.e., $\mu \le \mu_0$. Notice that

$$\rho_1\rho_2 = \frac{C}{A} = \frac{N(N+2)(N+3)}{(N+1)(2N+3)^2} f(\mu) \quad \text{with } f(\mu) = \frac{3\mu + 2(N+1)(N+3)}{3\mu + 2N(N+2)}. \tag{2.11}$$

It is clear that $f'(\mu) = -\frac{6(2N+3)}{(3\mu+2N^2+4N)^2} < 0$, so for all $\mu \le \mu_0$,

$$f(\mu_0) = -\frac{2N+5}{2N+1} \le f(\mu) \le f(-\infty) = 1.$$

Therefore,

$$-\frac{(N+2)(N+3)^2}{(N+1)(2N+3)^2} = \rho_{\min}\rho_{\max} < \rho_1\rho_2 < \rho_{\max}^2 = \left(\frac{N+3}{2N+3}\right)^2,$$

which implies that the smallest modulus of ρ_1 and ρ_2 must belong to $(\rho_{\min}, \rho_{\max})$. If $\mu = \mu_0$ (i.e., $g(\rho_{\min})g(\rho_{\max}) = 0$), there exists only one root $\rho = \rho_1 \in (\rho_{\min}, \rho_{\max})$, and the other one is $\rho_{\max}$ or $\rho_{\min}$. On the other hand, if $\mu < \mu_0$ (i.e., $g(\rho_{\min})g(\rho_{\max}) > 0$), both $\rho_1, \rho_2 \in (\rho_{\min}, \rho_{\max})$. In other words, when $\mu < \mu_0$, there are two quasi-orthogonal polynomials (corresponding to two roots of (2.7)) satisfying the requirements (a) and (b). In this case, we choose the one with the smallest modulus, which provides a more desirable distribution of the nodes and better approximations (cf. Remark 2.1). More precisely, we choose

$$\rho = \begin{cases} \rho_2 = \frac{-B-\sqrt{B^2-4AC}}{2A}, & \mu < \mu_1, \ \text{(or equivalently, } B < 0), \\ \rho_1 = \frac{-B+\sqrt{B^2-4AC}}{2A}, & \mu_1 \le \mu \le \mu_0, \ \text{(or equivalently, } B \ge 0), \end{cases} \tag{2.12}$$

where μ_0 is given by (2.10), and

$$\mu_1 = -\frac{4N^4 + 24N^3 + 50N^2 + 42N + 9}{6(N^2 + 3N + 3)}.$$

For clarity of presentation, we summarize the above analysis in the following lemma.

Lemma 2.1 *Let ρ be the root of the quadratic equation (2.7) selected according to*

- *if $\mu = -\frac{2}{3}N(N+2)$, ρ is given by (2.8);*
- *for $\mu \neq -\frac{2}{3}N(N+2)$,*
  - *if $\mu > \mu_0 = -\frac{2}{3}N^2 - 2N - \frac{1}{3}$, $\rho = \rho_1$ in (2.9);*
  - *if $\mu \leq \mu_0 = -\frac{2}{3}N^2 - 2N - \frac{1}{3}$, ρ is given by (2.12).*

Then the quasi-orthogonal polynomial in (2.2) satisfies the conditions (a) *and* (b).

With the above preparations, we are now ready to construct the quadrature formula (2.1).

Theorem 2.1 *Let $x_0 = -1$ and let $\{x_j\}_{j=1}^N$ be the zeros of the polynomial*

$$Q_N(x) = \pi_N^{(2,1)}(x) + \rho \pi_{N-1}^{(2,1)}(x), \quad x \in [-1, 1], \tag{2.13}$$

where ρ is given in Lemma 2.1, and let $\{h_j\}_{j=0}^{N+1}$ be the Lagrange basis (cf. (2.17)) *associated with the data $\{\phi(x_j)\}_{j=0}^N$ and $\phi'(1) + \mu\phi(1)$. Define*

$$\omega_j = \int_{-1}^1 h_j(x)\,dx, \quad 0 \leq j \leq N+1, \tag{2.14}$$

and assume that

$$\mu \neq -\frac{Q_N'(1)}{Q_N(1)} - \frac{1}{2}. \tag{2.15}$$

Then the quadrature rule

$$\int_{-1}^1 \phi(x)dx = \phi(-1)\omega_0 + \sum_{j=1}^N \phi(x_j)\omega_j + (\phi'(1) + \mu\phi(1))\omega_{N+1}, \quad \forall \phi \in \mathbb{P}_{2N+1}, \tag{2.16}$$

is exact for all $\phi \in \mathbb{P}_{2N+1}$, and the weights $\omega_j > 0$, for $1 \leq j \leq N$.

Proof We first define

$$h_j(x) = \begin{cases} (1 + \xi_0(1+x))\frac{Q_N(x)}{Q_N(-1)}, & j = 0, \\ \frac{(1+x)(\xi_j(x-x_j) + (1+x_j)^{-1})Q_N(x)}{(x-x_j)Q_N'(x_j)}, & 1 \leq j \leq N, \\ \frac{(1+x)Q_N(x)}{2Q_N'(1) + (2\mu+1)Q_N(1)}, & j = N+1, \end{cases} \tag{2.17}$$

where

$$\xi_j = \begin{cases} -\frac{Q_N'(1) + \mu Q_N(1)}{2Q_N'(1) + (2\mu+1)Q_N(1)}, & j = 0, \\ \frac{2Q_N(1)}{(1-x_j)^2(1+x_j)(2Q_N'(1) + (2\mu+1)Q_N(1))} - \frac{1}{1-x_j^2}, & 1 \leq j \leq N. \end{cases} \tag{2.18}$$

Notice that the assumption (2.15) guarantees $2Q'_N(1) + (2\mu + 1)Q_N(1) \neq 0$. One verifies that $\{h_k\}_{j=0}^{N+1}$ form the Lagrange basis polynomials of $\mathbb{P}_{N+1}$, and there holds

$$\begin{aligned} &h_k(x_j) = \delta_{kj} \quad \text{and} \quad h'_k(1) + \mu h_k(1) = 0, \quad 0 \le k, j \le N, \\ &h_{N+1}(x_j) = 0, \quad 0 \le j \le N \quad \text{and} \quad h'_{N+1}(1) + \mu h_{N+1}(1) = 1. \end{aligned} \tag{2.19}$$

Therefore, for any $\phi \in \mathbb{P}_{N+1}$, we write

$$\phi(x) = \sum_{k=0}^{N} \phi(x_k) h_k(x) + (\phi'(1) + \mu\phi(1)) h_{N+1}(x).$$

By the definition (2.14), there holds the exactness

$$\int_{-1}^{1} \phi(x)\,dx = \sum_{k=0}^{N} \phi(x_k)\omega_k + (\phi'(1) + \mu\phi(1))\omega_{N+1}, \quad \forall \phi \in \mathbb{P}_{N+1}. \tag{2.20}$$

We next show that (2.20) is also valid for all $\phi \in \mathbb{P}_{2N+1}$. For this purpose, let $\Psi_N(x)$ be the same as defined in (2.4), and define

$$\Psi_m(x) = x^m (1-x)^2 (1+x) Q_N(x), \quad 0 \le m \le N-2.$$

It is clear that

$$\mathbb{P}_{2N+1} = \text{span}\{x^j,\ 0 \le j \le N+1;\ \Psi_N(x);\ \Psi_m(x),\ 0 \le m \le N-2\}.$$

For any $P \in \mathbb{P}_{2N+1}$, we write

$$P(x) = \sum_{m=0}^{N-2} a_m \Psi_m(x) + b\Psi_N(x) + R(x), \quad R \in \mathbb{P}_{N+1}. \tag{2.21}$$

We see that

$$\int_{-1}^{1} P(x)\,dx = \sum_{m=0}^{N-2} a_m \int_{-1}^{1} \Psi_m(x)\,dx + b\int_{-1}^{1} \Psi_N(x)\,dx + \int_{-1}^{1} R(x)\,dx = \int_{-1}^{1} R(x)\,dx, \tag{2.22}$$

where we used the orthogonal property of the Jacobi polynomials and (2.3) to derive that

$$\int_{-1}^{1} \Psi_m(x)\,dx = \int_{-1}^{1} \Psi_N(x)\,dx = 0.$$

Moreover, we have that

$$\Psi_N(-1) = \Psi_N(x_j) = \Psi'_N(1) + \mu\Psi_N(1) = 0, \quad 1 \le j \le N,$$

and likewise for Ψ_m. Therefore, by (2.20)–(2.22),

$$\int_{-1}^{1} P(x)\,dx = \int_{-1}^{1} R(x)\,dx = \sum_{k=0}^{N} R(x_k)\omega_k + (R'(1) + \mu R(1))\omega_{N+1}$$

$$= \sum_{k=0}^{N} P(x_k)\omega_k + (P'(1) + \mu P(1))\omega_{N+1}, \quad \forall P \in \mathbb{P}_{2N+1}. \tag{2.23}$$

Hence, the existence of (2.1) is shown.

Finally, taking

$$P(x) = (1-x)^2(1+x)\left(\frac{Q_N(x)}{x - x_j}\right)^2 \in \mathbb{P}_{2N+1}, \quad 1 \le j \le N,$$

in (2.23), we verify readily that $\omega_j > 0$, $1 \le j \le N$. □

Remark 2.1 We notice from the derivation of Lemma 2.1 that if $\mu < \mu_0$, ρ is not unique, and we choose the one with the smallest modulus (cf. [10]), which gives more desirable grid distribution. As a numerical illustration, we tabulate in Table 1 the smallest and largest interior nodes for $\rho = \rho_1, \rho_2$ and the Legendre-Gauss-Lobatto points, which shows that the choice ρ_1 yields reasonable distribution.

For a further justification, we test the quadrature formula (2.1) with $\phi(x) = e^x$, $\mu = (\mu_0 + \mu_1)/2$, μ_1, $\mu_1 - 100$ and various N, and plot the errors with $\rho = \rho_1, \rho_2$ in Figs. 1–3 against N, which indicates that in all cases, the choice of ρ in (2.12) provides much better approximations.

Table 1 The smallest and largest interior nodes

	$\rho = \rho_1$		$\rho = \rho_2$		Legendre-Gauss-Lobatto	
N	min(nodes)	max(nodes)	min(nodes)	max(nodes)	min(nodes)	max(nodes)
5	−0.82392404	0.93595738	−0.99914153	0.69481230	−0.83022389	0.83022389
50	−0.99723161	0.99900244	−0.99999978	0.99502965	−0.99723318	0.99723318
100	−0.99928740	0.99974325	−0.99999998	0.99872007	−0.99928750	0.99928750

Fig. 1 $\mu = \frac{\mu_0+\mu_1}{2}$

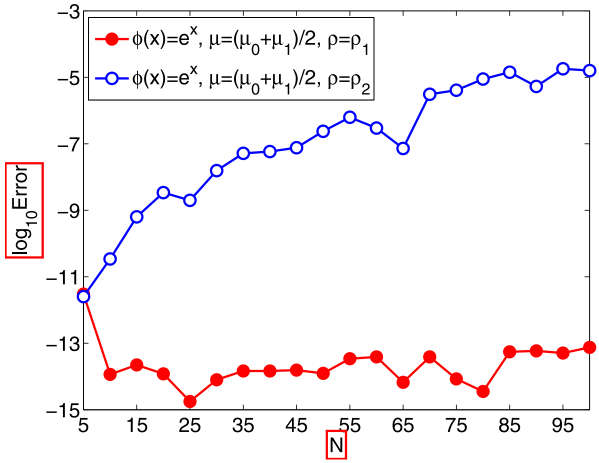

Fig. 2 $\mu = \mu_1$

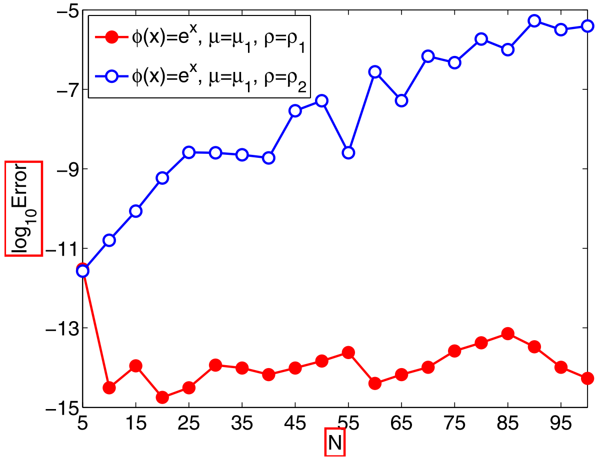

Fig. 3 $\mu = \mu_1 - 100 < \mu_1$

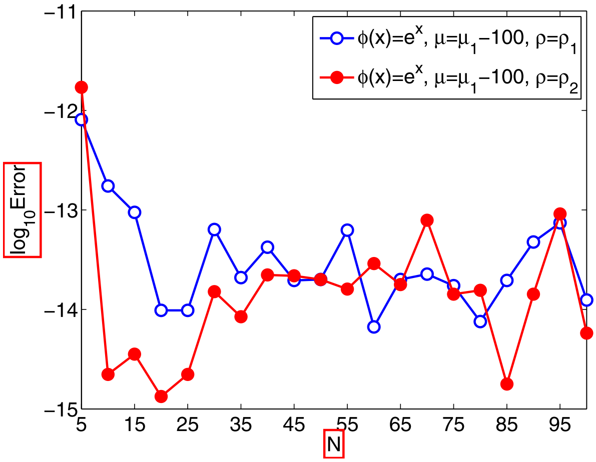

Remark 2.2 We point out that [10] provided a general framework for the existence of more general quadrature rules, but the direct application of the general results leads to severe constraint on the constant μ. However, the condition (2.15) is very mild. In fact, since $(1-x_j)^{-1} > \frac{1}{2}$, we have the rough estimate:

$$\mathcal{Q}(N,\mu) := -\frac{Q_N'(1)}{Q_N(1)} - \frac{1}{2} = -\sum_{j=1}^{N} \frac{1}{1-x_j} - \frac{1}{2} < -\frac{1}{2}(N+1), \quad \forall N \in \mathbb{N}, \ \forall \mu \in \mathbb{R}.$$

Hence, if $\mu \geq -\frac{1}{2}(N+1)$, then $\mu \neq \mathcal{Q}(N,\mu)$. Moreover, we verify that $\mu = \mathcal{Q}(N,\mu)$ is equivalent to

$$\mu^2 + B_0\mu + C_0 = 0, \tag{2.24}$$

where

$$B_0 = (3N^2 + 7N + 2)/3, \qquad C_0 = 2N(N^3 + 5N^2 + 8N + 4)/9.$$

Fig. 4 μ vs. N for $\mu = \mathcal{Q}(N, \mu)$

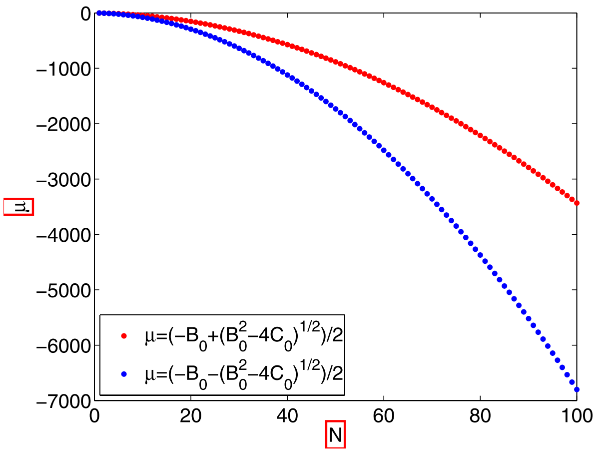

If μ is not the root of (2.24), then $\mu \neq \mathcal{Q}(N, \mu)$. We also observe that the quadratic equation (2.24) has two negative roots. We plot in Fig. 4 the graph of two roots of $\mu = \mathcal{Q}(N, \mu)$ for $N \in [1, 100]$. We see that for given μ, there exist at most two different values of N, such that $\mu = \mathcal{Q}(N, \mu)$.

2.2 Evaluation of the Nodes and Weights

Following Theorem 3.3 of [10], we can evaluate the nodes by the well-known eigen-method of Golub and Welsch [12]. One verifies that the quasi-orthogonal polynomial $Q_N(x)$ has the following matrix representation:

$$Q_N(x) = \det(x\mathbb{I}_N - \mathbb{J}_N), \tag{2.25}$$

where $\mathbb{I}_N$ is the $N \times N$ identity matrix, and $\mathbb{J}_N$ is a symmetric tri-diagonal matrix of order N,

$$\mathbb{J}_N = \begin{bmatrix} \alpha_0 & \sqrt{\beta_1} & & & \\ \sqrt{\beta_1} & \alpha_1 & \sqrt{\beta_2} & & \\ & \ddots & \ddots & \ddots & \\ & & \sqrt{\beta_{N-2}} & \alpha_{N-2} & \sqrt{\beta_{N-1}} \\ & & & \sqrt{\beta_{N-1}} & \alpha_{N-1} - \rho \end{bmatrix} \tag{2.26}$$

with α_n and β_n given by (cf. (A.9))

$$\alpha_n = -\frac{3}{(2n+3)(2n+5)}, \qquad \beta_n = \frac{n(n+3)}{(2n+3)^2}.$$

Thus, the interior nodes $\{x_j\}_{j=1}^N$ of the quadrature formula (2.16) are the eigenvalues of $\mathbb{J}_N$, which can be evaluated efficiently using, e.g., the QR-algorithm as with the classical Gauss-type quadrature. Alternatively, we may employ the iterative methods such as Newton-Raphson's method using the zeros of $\pi_N^{(2,1)}(x)$ as the initial approximation.

The weights can be computed explicitly by formulas derived in Appendix B. Some samples of nodes and weights computed by the above algorithm are given in Appendix B.

3 Collocation Methods for Linear Problems

In this section, we implement the collocation methods based on the quadrature formula (2.1) for second-order equations with mixed Dirichlet-Robin boundary conditions. We begin with a one-dimensional model equation and a two-dimensional convection-diffusion equation.

3.1 One-dimensional Problem

We first consider

$$\begin{cases} -\varepsilon u''(x)+p(x)u'(x)+q(x)u(x)=f(x), \quad \varepsilon>0,\ x\in(-1,1), \\ u(-1)=g_-, \qquad u'(1)+\mu u(1)=g_+, \end{cases} \tag{3.1}$$

where $p, q, f, g_\pm$ and μ are given data.

3.1.1 Collocation Scheme

Let $\{x_j\}_{j=1}^N$ be the interior quadrature nodes in (2.1). The collocation approximation to (3.1) is to find $u_N \in \mathbb{P}_{N+1}$ such that

$$\begin{cases} -\varepsilon u_N''(x_j)+p(x_j)u_N'(x_j)+q(x_j)u_N(x_j)=f(x_j), \quad 1\le j\le N, \\ u_N(-1)=g_-, \qquad u_N'(1)+\mu u_N(1)=g_+. \end{cases} \tag{3.2}$$

We now examine the matrix form of this scheme. Let $\{h_j\}_{j=0}^{N+1}$ be the Lagrangian basis polynomials defined in (2.17)–(2.18). Under this nodal basis, we write

$$u_N(x)=g_-h_0(x)+g_+h_{N+1}(x)+\sum_{k=1}^N a_k h_k(x)\in\mathbb{P}_{N+1}. \tag{3.3}$$

Thanks to (2.19), we have $u_N(-1)=g_-$, $u_N'(1)+\mu u_N(1)=g_+$ and $u_N(x_k)=a_k$, $1\le k\le N$. The system of (3.2) becomes

$$\mathbf{A}_c\vec{\mathbf{a}} := (-\varepsilon \mathbf{D}_{\rm in}^{(2)}+\mathbf{p}\mathbf{D}_{\rm in}^{(1)}+\mathbf{q})\vec{\mathbf{a}}=\vec{\mathbf{b}}, \tag{3.4}$$

where

$$\begin{aligned} &d_{jk}^{(i)}=h_k^{(i)}(x_j), \quad 0\le j,k\le N+1, \qquad \mathbf{D}_{\rm in}^{(i)}=(d_{jk}^{(i)})_{1\le j,k\le N},\ i=1,2; \\ &\mathbf{p}=\mathrm{diag}(p(x_1),p(x_2),\ldots,p(x_N)), \\ &\mathbf{q}=\mathrm{diag}(q(x_1),q(x_2),\ldots,q(x_N)), \qquad \vec{\mathbf{a}}=(a_1,a_2,\ldots,a_N)^T, \\ &\vec{\mathbf{b}}=(f(x_1),\ldots,f(x_N))^T+\varepsilon(d_{10}^{(2)},d_{20}^{(2)},\ldots,d_{N0}^{(2)})^T g_- \\ &\qquad +\varepsilon(d_{1(N+1)}^{(2)},d_{2(N+1)}^{(2)},\ldots,d_{N(N+1)}^{(2)})^T g_+ \\ &\qquad -\mathbf{p}(d_{10}^{(1)},d_{20}^{(1)},\ldots,d_{N0}^{(1)})^T g_- -\mathbf{p}(d_{1(N+1)}^{(1)},d_{2(N+1)}^{(1)},\ldots,d_{N(N+1)}^{(1)})^T g_+. \end{aligned} \tag{3.5}$$

It is seen that like the Legendre-Gauss-Lobatto (LGL) collocation method for Dirichlet problems, the numerical solution satisfies the boundary conditions exactly, and the proposed method is easy to implement once the associated differentiation matrices are pre-computed.

It is known that the mth order LGL differentiation matrix equals to that of the first-order to power m. Although this property is not available for this case, we can compute the higher-order differentiation matrices in a recursive fashion.

Lemma 3.1 *Let*

$$d_{jk}^{(l)} = h_k^{(l)}(x_j) = \frac{d^l h_k}{dx^l}(x_j), \qquad \mathbf{D}^{(l)} = (d_{jk}^{(l)})_{0\le j,k\le N+1}, \quad l \ge 1. \tag{3.6}$$

Then we have

$$\begin{cases} \mathbf{D}^{(l+1)} = \mathbf{D}^{(1)} \times \widetilde{\mathbf{D}}^{(l)}, & l \ge 0, \\ \mathbf{D}^{(0)} = \widetilde{\mathbf{D}}^{(0)} = \mathbb{I}_{N+2}, \end{cases} \tag{3.7}$$

where $\mathbb{I}_{N+2}$ is the identity matrix, and $\widetilde{\mathbf{D}}^{(l)}$ is identical to $\mathbf{D}^{(l)}$ except that the last row of $\mathbf{D}^{(l)}$ is replaced by

$$\big(d_{(N+1)0}^{(l+1)} + \mu d_{(N+1)0}^{(l)}, d_{(N+1)1}^{(l+1)} + \mu d_{(N+1)1}^{(l)}, \ldots, d_{(N+1)(N+1)}^{(l+1)} + \mu d_{(N+1)(N+1)}^{(l)}\big).$$

Proof For any $\phi \in \mathbb{P}_{N+1}$, we have that

$$\phi(x) = \phi(-1)h_0(x) + \sum_{j=1}^{N} \phi(x_j)h_j(x) + (\phi'(1) + \mu\phi(1))h_{N+1}(x),$$

which implies

$$\phi'(x) = \phi(-1)h_0'(x) + \sum_{j=1}^{N} \phi(x_j)h_j'(x) + (\phi'(1) + \mu\phi(1))h_{N+1}'(x).$$

Let $x_0 = -1$ and $x_{N+1} = 1$. Taking $\phi(x) = h_k^{(l)}(x)$ and $x = x_i$ leads to that for all $0 \le i, k \le N+1$ and $l \ge 1$,

$$\begin{aligned} d_{ik}^{(l+1)} = h_k^{(l+1)}(x_i) &= h_k^{(l)}(x_0)h_0'(x_i) + \sum_{j=1}^{N} h_k^{(l)}(x_j)h_j'(x_i) \\ &\quad + \big(h_k^{(l+1)}(x_{N+1}) + \mu h_k^{(l)}(x_{N+1})\big)h_{N+1}'(x_i) \\ &= d_{i0}^{(1)}d_{0k}^{(l)} + \sum_{j=1}^{N} d_{ij}^{(1)}d_{jk}^{(l)} + d_{i(N+1)}^{(1)}\big(d_{(N+1)k}^{(l+1)} + \mu d_{(N+1)k}^{(l)}\big), \end{aligned} \tag{3.8}$$

which leads to the desired result. □

As a consequence of this lemma, it suffices to evaluate the first-order differentiation matrix $\mathbf{D}^{(1)}$ and values $h_k^{(l+1)}(1)$ for $l \ge 1$ and $0 \le k \le N+1$ to compute higher-order differentiation matrices.

3.1.2 Numerical Results

We first compare the collocation method with the standard approach using Legendre-Gauss-Lobatto (LGL) points. Let $\xi_0 = -1,\ \xi_{N+1} = 1$ and $\{\xi_j\}_{j=1}^N$ be the zeros of $L_{N+1}'(\xi)$, where

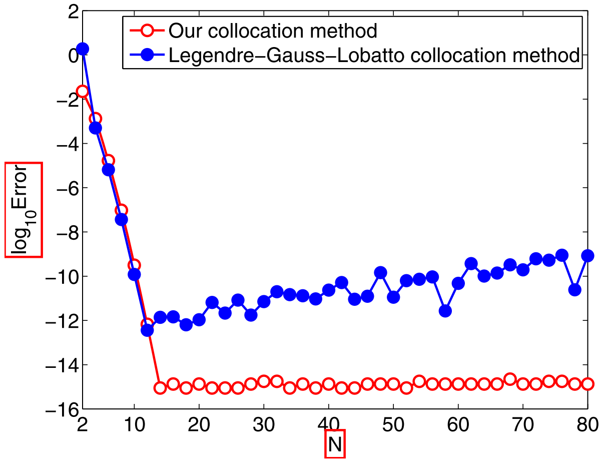

Fig. 5 L^∞-errors of Example 1

L_{N+1} is the Legendre polynomial of degree $N+1$. The LGL collocation scheme for (3.1) is to find $v_N \in \mathbb{P}_{N+1}$ such that

$$\begin{cases} -\varepsilon v_N''(\xi_j) + p(\xi_j)v_N'(\xi_j) + q(\xi_j)v_N(\xi_j) = f(\xi_j), \quad 1 \le j \le N, \\ v_N(\xi_0) = g_-, \quad v_N'(\xi_{N+1}) + \mu v_N(\xi_{N+1}) = g_+. \end{cases} \tag{3.9}$$

In contrast with the scheme (3.2), the boundary value $v_N(-1)$ is treated as an unknown.

Example 1 Taking $\varepsilon = 1$, $p(x) \equiv 0$, $q(x) \equiv 1$ and $\mu = 1$ in (3.1), we test the exact solution $u(x) = (x+2)e^{-x}$ on two schemes (3.2) and (3.9). In Fig. 5, we plot the maximum pointwise errors, and find that the standard LGL collocation method suffers from much severe roundoff errors, while the new collocation method is stable even for large N.

Next, we further test the collocation scheme (3.2) on several examples.

Example 2 We take $\varepsilon = 1$, $p(x) \equiv 0$ and various $q(x)$, and test an oscillatory solution: $u(x) = \cos^2(12\pi x)$. In Figs. 6 and 7, we plot the discrete L^∞- and L^2-errors with $\mu = 1, 0$ and $q(x) = 1,\ 100 + \sin(100\pi x)$, respectively. We also visualize a convergence rate $O(e^{-cN})$ for some $c > 0$.

Example 3 We take $p(x) = -2x$, $q(x) \equiv 0$, $\mu = 1$ and various ε, and test the exact solution $u(x) = \mathrm{erf}(x/\sqrt{\varepsilon})$, which has a steep front at $x = 0$ as $\varepsilon \ll 1$. In Fig. 8, we plot the discrete L^∞-errors. We find that scheme (3.2) provides a fairly good numerical approximation for large N and small ε, and observe that more points are needed to resolve the transition layer at $x = 0$ for very small ε.

Example 4 We take $\varepsilon = 1$, $p(x) \equiv 0$, $q(x) \equiv 1$ and $\mu = 1$, and test the exact solution $u(x) = (1+x)^\gamma e^x$, where $\gamma > \frac{1}{2}$ is a non-integer. Hence, the solution has a finite regularity. In Fig. 9, we plot the discrete L^2-errors against various N with $\gamma = 1.1, 2.1, 3.1, 4.1$, which also shows that the proposed method provides an accurate approximation. The observed convergence rates for the L^2-errors are of $O(N^{-2\gamma})$, which is slightly slower than the

Fig. 6 L^∞-errors of Example 2

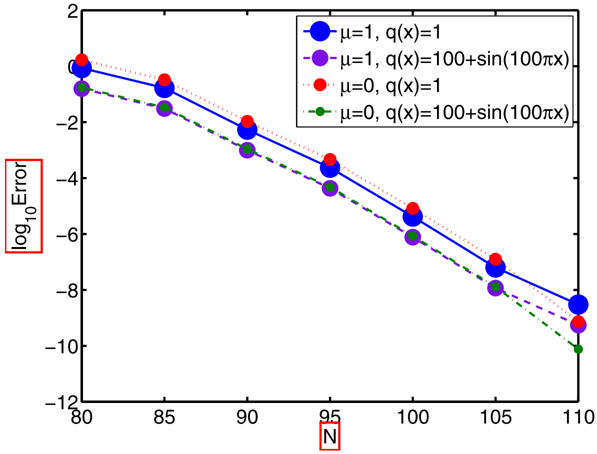

Fig. 7 L^2-errors of Example 2

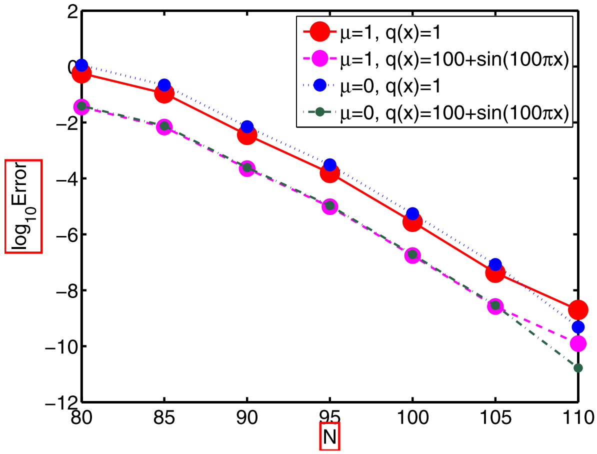

Fig. 8 L^∞-errors of Example 3

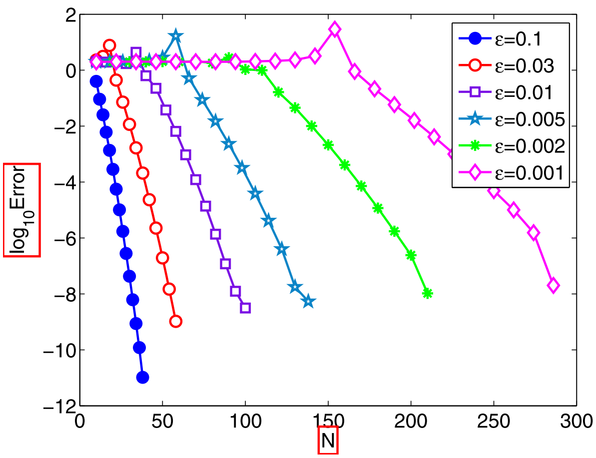

Fig. 9 L^2-errors of Example 4

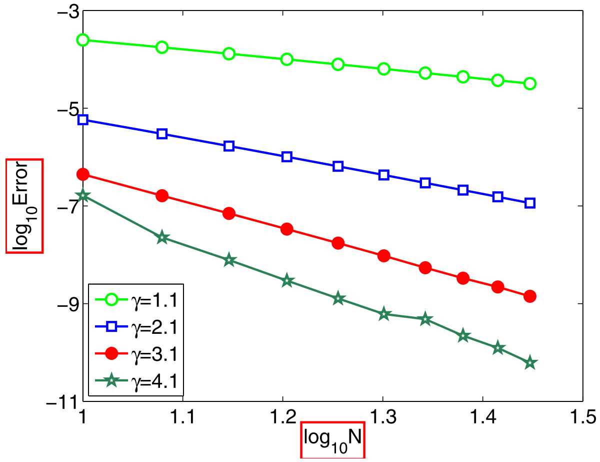

Fig. 10 L^∞-errors of scheme (3.12)

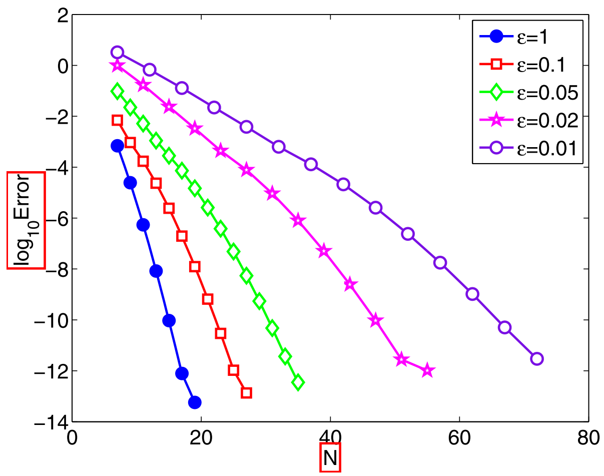

Legendre-Gauss-Lobatto for Dirichlet problems, where a convergence rate $O(N^{-2\gamma-1+\epsilon})$ for some small $\epsilon > 0$.

3.1.3 A Finite-difference Preconditioner

Although the collocation scheme (3.2) is easy to implement, the coefficient matrix $\mathbf{A}_c$ is full with $\mathrm{Cond}(\mathbf{A}_c) \sim N^4$, and thereby when N is large, the direct inversion of the systems may suffer from severe roundoff errors. To overcome this trouble, it is advisable to construct a preconditioning for the system (3.4), and use a suitable iteration solver [5, 8]. Canuto [5] proposed a finite-difference preconditioning for the LGL collocation method for Neumann problems, and Sun et al. [23] developed an interesting preconditioning for Hermite cubic collocation methods. However, these techniques can not be applied to this context directly. Here, we use a different treatment of boundary conditions to derive an optimal finite difference preconditioner as that in [5]. More precisely, assume that $\{x_j\}_{j=0}^{N+1}$ (with $x_0 = -1$ and

Table 2 The spectral radii of $\mathbf{A}_c$ and $\mathbf{A}_d^{-1}\mathbf{A}_c$

N	$\mathbf{A}_c$	$\mathbf{A}_d^{-1}\mathbf{A}_c$	$\mathbf{A}_c$	$\mathbf{A}_d^{-1}\mathbf{A}_c$
8	219.3	1.92	318.7	1.35
16	2415.0	2.17	2514.8	1.78
32	32040.8	2.31	32140.6	2.14
64	466760.4	2.39	466860.0	2.33
128	7125970.9	2.42	7126070.1	2.41
256	111373205.5	2.44	111373304.5	2.44
512	1761205287.4	2.45	1761205386.4	2.45

$x_{N+1} = 1$) are arranged in the ascending order. We use central differences with three stencils at the points $\{x_j\}_{j=1}^{N-1}$, and discretize $u'(x_N)$ and $u''(x_N)$ specially as

$$\begin{cases} u'(x_N) \approx \frac{u_N - u_{N-1} + \delta_N(u'(1)+\mu u(1) - \mu u_N)}{2\delta_N} = \frac{-u_{N-1} + (1-\mu\delta_N)u_N + \delta_N g_+}{2\delta_N}, \\ u''(x_N) \approx \frac{u_{N-1} - u_N + \delta_N(u'(1)+\mu u(1) - \mu u_N)}{\delta_N(\delta_N/2+\delta_{N+1})} = \frac{u_{N-1} - (1+\mu\delta_N)u_N + \delta_N g_+}{\delta_N(\delta_N/2+\delta_{N+1})}, \end{cases} \tag{3.10}$$

where u_j is the finite difference approximation of $u(x_j)$, and $\delta_j = x_j - x_{j-1}$.

Denote by $\mathbf{A}_d$ the resultant coefficient matrix of the finite difference method, and the preconditioner $\mathbf{A}_d^{-1}$ can be regarded as an approximation of the inverse of $\mathbf{A}_c$. Table 2 contains the spectral radii (i.e., the largest modulus of the eigenvalues) of $\mathbf{A}_c$ (cf. (3.4)) and $\mathbf{A}_d^{-1}\mathbf{A}_c$ with $\varepsilon = 1$, $\mu = 1$, $p(x) \equiv 0$, $q(x) \equiv 1$ (in columns 2–3) and $q(x) = 100 + \sin(100\pi x)$ (in columns 4–5). The eigenvalues of two matrices are real, positive and distinct in all cases. We also point out that the smallest modulus of the eigenvalues of $\mathbf{A}_d^{-1}\mathbf{A}_c$ is larger than 0.95 for both cases, while that of $\mathbf{A}_c$ is 2.3 for $q(x) \equiv 1$ and 101 for $q(x) = 100 + \sin(100\pi x)$. The eigenvalues of the preconditioned matrix $\mathbf{A}_d^{-1}\mathbf{A}_c$ lie in the interval $[0.95, 2.5]$, as shown in Table 2, and therefore the system (3.4) can be solved efficiently by an iteration solver.

In Figs. 11 and 12, we plot the eigenvalue distributions of $\mathbf{A}_c$ and $\mathbf{A}_d^{-1}\mathbf{A}_c$ with $p(x) = -2x$, $q(x) \equiv 0$, $\mu = 1$ and $\varepsilon = 0.002$. It is clear that for all N, the preconditioned matrix $\mathbf{A}_d^{-1}\mathbf{A}_c$ has much smaller magnitude, and the real parts of its eigenvalues are always positive. Hence, the preconditioning significantly leads to a well-conditioned system (3.4) for an effective iterative solver.

3.2 Two-dimensional Problem

We next consider the convection-diffusion equation (cf. [20]):

$$\begin{cases} \varepsilon^{-1}\partial_x u(x,y) = \partial_x^2 u(x,y) + \partial_y^2 u(x,y) + f(x,y), & \varepsilon > 0,\ x, y \in (-1,1), \\ u(-1,y) = g_-(y), \quad \partial_x u(1,y) + \mu_1 u(1,y) = g_+(y), & y \in [-1,1], \\ u(x,-1) = h_-(x), \quad \partial_y u(x,1) + \mu_2 u(x,1) = h_+(x), & x \in [-1,1], \end{cases} \tag{3.11}$$

where $f, g_\pm, h_\pm, \mu_1$ and μ_2 are given data. Moreover, $g_\pm(y)$ and $h_\pm(x)$ satisfy the compatibility conditions at the corners.

3.2.1 Collocation Scheme

Let $x_0 = y_0 = -1$, $x_{M+1} = y_{N+1} = 1$, and $\{x_k\}_{k=1}^M$ and $\{y_j\}_{j=1}^N$ be the interior quadrature nodes in (2.1) with $\mu = \mu_1, \mu_2$, respectively. The collocation approximation to (3.11) is to

Fig. 11 Eigenvalue distributions of $\mathbf{A}_{\mathrm{c}}$

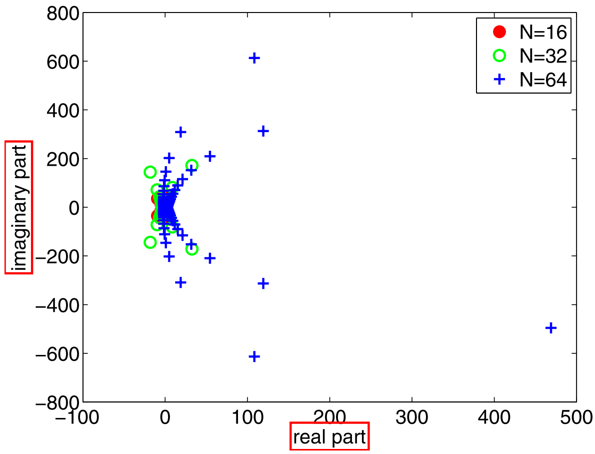

Fig. 12 Eigenvalue distributions of $\mathbf{A}_{\mathrm{d}}^{-1}\mathbf{A}_{\mathrm{c}}$

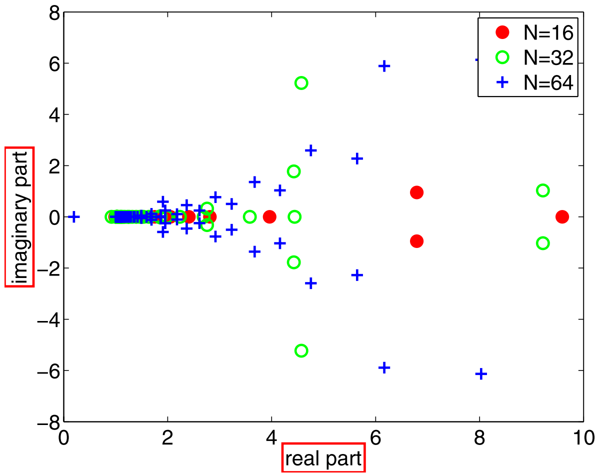

find $u_{M,N}(x,y) \in \mathbb{P}_{M+1}(-1,1) \otimes \mathbb{P}_{N+1}(-1,1)$ such that

$$\begin{cases} \varepsilon^{-1}\partial_x u_{M,N}(x_k,y_j) = \partial_x^2 u_{M,N}(x_k,y_j) + \partial_y^2 u_{M,N}(x_k,y_j) + f(x_k,y_j), \\ \quad 1 \le k \le M,\ 1 \le j \le N, \\ u_{M,N}(-1,y_j) = g_-(y_j), \quad 0 \le j \le N+1, \\ \partial_x u_{M,N}(1,y_j) + \mu_1 u_{M,N}(1,y_j) = g_+(y_j), \quad 1 \le j \le N+1, \\ u_{M,N}(x_k,-1) = h_-(x_k), \quad 1 \le k \le M+1, \\ \partial_y u_{M,N}(x_k,1) + \mu_2 u_{M,N}(x_k,1) = h_+(x_k), \quad 1 \le k \le M. \end{cases} \tag{3.12}$$

We now examine the matrix form of this scheme. Let $\{\hat{h}_m(x)\}_{m=0}^{M+1}$ and $\{\tilde{h}_n(y)\}_{n=0}^{N+1}$ be the Lagrangian basis polynomials defined in (2.17)–(2.18) with $\mu = \mu_1, \mu_2$, respectively. We write

$$u_{M,N}(x,y) = \sum_{m=0}^{M+1}\sum_{n=0}^{N+1} a_{m,n}\hat{h}_m(x)\tilde{h}_n(y). \tag{3.13}$$

Thanks to (2.19) and (3.12), we have

$$\begin{cases} a_{0,n} = g_-(y_n), & 0 \le n \le N, \quad a_{0,N+1} = g_-(1)/\tilde{h}_{N+1}(1), \\ a_{m,0} = h_-(x_m), & 1 \le m \le M, \quad a_{M+1,0} = h_-(1)/\hat{h}_{M+1}(1), \\ a_{M+1,n} = g_+(y_n), & 1 \le n \le N, \quad a_{M+1,N+1} = (g_+(1) - \sum_{n=0}^{N} g_+(y_n)\tilde{h}_n(1))/\tilde{h}_{N+1}(1), \\ a_{m,N+1} = h_+(x_m), & 1 \le m \le M. \end{cases} \tag{3.14}$$

Moreover, $u_{M,N}(x_k, y_j) = a_{k,j}$, $1 \le k \le M$, $1 \le j \le N$. Next, let

$$\mathbb{A}_k = \begin{bmatrix} \hat{h}_1^{(k)}(x_1) & \hat{h}_2^{(k)}(x_1) & \dots & \hat{h}_M^{(k)}(x_1) \\ \hat{h}_1^{(k)}(x_2) & \hat{h}_2^{(k)}(x_2) & \dots & \hat{h}_M^{(k)}(x_2) \\ \vdots & \vdots & & \vdots \\ \hat{h}_1^{(k)}(x_M) & \hat{h}_2^{(k)}(x_M) & \dots & \hat{h}_M^{(k)}(x_M) \end{bmatrix}, \quad k = 0, 1, 2, \tag{3.15}$$

and

$$\mathbb{B}_k = \begin{bmatrix} \tilde{h}_1^{(k)}(y_1) & \tilde{h}_2^{(k)}(y_1) & \dots & \tilde{h}_N^{(k)}(y_1) \\ \tilde{h}_1^{(k)}(y_2) & \tilde{h}_2^{(k)}(y_2) & \dots & \tilde{h}_N^{(k)}(y_2) \\ \vdots & \vdots & & \vdots \\ \tilde{h}_1^{(k)}(y_N) & \tilde{h}_2^{(k)}(y_N) & \dots & \tilde{h}_N^{(k)}(y_N) \end{bmatrix}, \quad k = 0, 2, \tag{3.16}$$

Clearly, $\mathbb{A}_0 = \mathbb{I}_M$ and $\mathbb{B}_0 = \mathbb{I}_N$. We also denote by

$$\mathbb{A} = (\varepsilon^{-1}\mathbb{A}_1 - \mathbb{A}_2) \otimes \mathbb{B}_0 - \mathbb{A}_0 \otimes \mathbb{B}_2.$$

Then the system of (3.12) becomes

$$\mathbb{A}\vec{\mathbf{a}} = \vec{\mathbf{b}}, \tag{3.17}$$

where

$$\begin{aligned} \vec{\mathbf{a}} &= (a_{1,1}, a_{1,2}, \dots, a_{1,N}, \dots, a_{M,1}, a_{M,2}, \dots, a_{M,N})^T, \\ \vec{\mathbf{b}} &= (b_{1,1}, b_{1,2}, \dots, b_{1,N}, \dots, b_{M,1}, b_{M,2}, \dots, b_{M,N})^T, \end{aligned} \tag{3.18}$$

with

$$\begin{aligned} b_{k,j} = {} & f(x_k, y_j) - \varepsilon^{-1} a_{0,j}\hat{h}_0'(x_k) + a_{0,j}\hat{h}_0''(x_k) + a_{k,0}\tilde{h}_0''(y_j) \\ & - \varepsilon^{-1} a_{M+1,j}\hat{h}_{M+1}'(x_k) + a_{M+1,j}\hat{h}_{M+1}''(x_k) + a_{k,N+1}\tilde{h}_{N+1}''(y_j), \\ & 1 \le k \le M, \ 1 \le j \le N. \end{aligned}$$

3.2.2 Numerical Results

To examine the accuracy of the above scheme, we take $\mu_1 = 1$, $\mu_2 = 2$ and various ε in (3.12), and test the exact solution $u(x) = (1 - e^{(x-1)/\varepsilon})\sin(\pi y)$. The solution has a steep front along the line $x = 1$ as $\varepsilon \ll 1$. In Fig. 10, we plot the discrete L^∞-errors with $M = N$, and visualize a convergence behavior similar to the one-dimensional cases.

4 Applications to the Helmholtz Equation

In this section, we apply the collocation methods described in the previous section to the time-harmonic wave scattering governed by the Helmholtz equation. Let $D = \{(r,\theta) \mid 0 \le r \le r_0,\ 0 \le \theta \le 2\pi\}$ be the scatter. We consider the Helmholtz equation with the Sommerfeld radiation condition at infinity:

$$\begin{cases} \Delta w(r,\theta) + k^2 w(r,\theta) = f(r,\theta), & (r,\theta) \in \mathbb{R}^2 \setminus \bar{D}, \\ w(r_0,\theta) = w_0(\theta), & \theta \in [0,2\pi], \\ \partial_r w(r,\theta) - \mathrm{i}kw(r,\theta) = o(r^{-\frac{1}{2}}), & \text{as } r \to \infty,\ \theta \in [0,2\pi], \end{cases} \tag{4.1}$$

where k is the wave-number, and Δ is Laplace operator in polar coordinates. Such a problem presents a great challenge for numerical computations due to (i) the unbounded computational domain, and (ii) highly oscillatory solution when $k \gg 1$. There has been extensive research work devoted to overcoming these difficulties (see, e.g., [2, 14] and the references therein). Here, we adopt the Dirichlet-to-Neumann (DtN) technique (cf. [17, 21]) for domain truncation, and apply the collocation methods described in the previous section to the resulting problem in the bounded domain. Such a combined approach appears to be particularly robust for moderate to high wave numbers, and therefore provides a viable alternative for the spectral-Galerkin approach in [22].

We truncate the computational domain by a circle of radius r_1 such that the support of the source term f is enclosed in the bounded domain

$$\Omega := \{(r,\theta) : r_0 < r < r_1,\ 0 \le \theta \le 2\pi\}. \tag{4.2}$$

By the method of separation of variables, the Helmholtz equation: $\Delta w + k^2 w = 0$ exterior to the artificial circle $r = r_1$ can be solved analytically, and the exact solution is

$$w(r,\theta) = \sum_{|m|=0}^{\infty} \frac{H_m^{(1)}(kr)}{H_m^{(1)}(kr_1)} \hat{w}_m(r_1) e^{\mathrm{i}m\theta}, \quad (r,\theta) \in [r_1,\infty) \times [0,2\pi], \tag{4.3}$$

where $H_m^{(1)}(z)$ is the Hankel function of the first kind of order m, and $\hat{w}_m(r_1)$ is the coefficient of the Fourier expansion of $w(r_1,\theta)$ in the periodic direction. We define the DtN operator by

$$\boldsymbol{T} w(r_1,\theta) = -\partial_r w(r_1,\theta) = -\sum_{|m|=0}^{\infty} k \frac{H_m^{(1)'}(kr_1)}{H_m^{(1)}(kr_1)} \hat{w}_m(r_1) e^{\mathrm{i}m\theta}, \quad \theta \in [0,2\pi]. \tag{4.4}$$

Consequently, we can reduce the problem (4.1) in unbounded domain to

$$\begin{cases} \Delta w(r,\theta) + k^2 w(r,\theta) = f(r,\theta), & (r,\theta) \in \Omega, \\ w(r_0,\theta) = w_0(\theta), & \theta \in [0,2\pi], \\ (\partial_r w(r,\theta) + \boldsymbol{T} w(r,\theta))|_{r=r_1} = 0, & \theta \in [0,2\pi]. \end{cases} \tag{4.5}$$

Using the Fourier expansion in the periodic direction,

$$\{w(r,\theta), f(r,\theta), w_0(\theta)\} = \sum_{|m|=0}^{\infty} \{\hat{w}_m(r), \hat{f}_m(r), \hat{g}_m\} e^{\mathrm{i}m\theta}, \tag{4.6}$$

we obtain a sequence of one-dimensional problems:

$$\begin{cases} \frac{1}{r}(r\hat{w}_m'(r))' + \left(k^2 - \frac{m^2}{r^2}\right)\hat{w}_m(r) = \hat{f}_m(r), & r \in (r_0, r_1), \\ \hat{w}_m(r_0) = \hat{g}_m, \qquad \hat{w}_m'(r_1) + \mathcal{T}_{m,k}\hat{w}_m(r_1) = 0, \end{cases} \tag{4.7}$$

where

$$\mathcal{T}_{m,k} = -k \frac{H_m^{(1)'}(kr_1)}{H_m^{(1)}(kr_1)}. \tag{4.8}$$

In order to separate the complex mixed boundary conditions, we make the transform

$$\{\hat{w}_m(r), \hat{f}_m(r)\} = e^{-r\mathcal{T}_{m,k}}\{\tilde{w}_m(r), \tilde{f}_m(r)\}, \qquad \hat{g}_m = e^{-r_0\mathcal{T}_{m,k}}\tilde{g}_m. \tag{4.9}$$

This allows us to convert (4.7) into

$$\begin{cases} \tilde{w}_m''(r) + \left(\frac{1}{r} - 2\mathcal{T}_{m,k}\right)\tilde{w}_m'(r) + \left(k^2 - \frac{m^2}{r^2} + \mathcal{T}_{m,k}^2 - \frac{1}{r}\mathcal{T}_{m,k}\right)\tilde{w}_m(r) = \tilde{f}_m(r), \\ \tilde{w}_m(r_0) = \tilde{g}_m, \qquad \tilde{w}_m'(r_1) = 0. \end{cases} \tag{4.10}$$

We now map the interval $[r_0, r_1]$ to $[-1, 1]$ for ease of implementing the collocation methods:

$$r = \frac{(r_1 - r_0)x + r_1 + r_0}{2}, \qquad x \in [-1, 1],$$

and denote

$$\{\tilde{w}_{R,m}(x), \tilde{w}_{I,m}(x)\} = \{\mathrm{Re}\tilde{w}_m(r), \mathrm{Im}\tilde{w}_m(r)\},$$

(likewise for $\tilde{f}_{R,m}(x)$, $\tilde{f}_{I,m}(x)$, $\tilde{g}_{R,m}$ and $\tilde{g}_{I,m}$). Then we rewrite (4.10) as

$$\begin{cases} \frac{4}{(r_1-r_0)^2}\tilde{w}_{R,m}'' + \frac{2}{r_1-r_0}(a_0\tilde{w}_{R,m}' - b_0\tilde{w}_{I,m}') + a_1\tilde{w}_{R,m} - b_1\tilde{w}_{I,m} = \tilde{f}_{R,m}, & x \in (-1,1), \\ \frac{4}{(r_1-r_0)^2}\tilde{w}_{I,m}'' + \frac{2}{r_1-r_0}(b_0\tilde{w}_{R,m}' + a_0\tilde{w}_{I,m}') + b_1\tilde{w}_{R,m} + a_1\tilde{w}_{I,m} = \tilde{f}_{I,m}, & x \in (-1,1), \\ \tilde{w}_{R,m}(-1) = \tilde{g}_{R,m}, \qquad \tilde{w}_{R,m}'(1) = 0, \qquad \tilde{w}_{I,m}(-1) = \tilde{g}_{I,m}, \qquad \tilde{w}_{I,m}'(1) = 0, \end{cases} \tag{4.11}$$

where

$$a_0(x) = \frac{2}{(r_1 - r_0)x + r_1 + r_0} - 2\,\mathrm{Re}\,\mathcal{T}_{m,k}, \qquad b_0 = -2\mathrm{Im}\,\mathcal{T}_{m,k},$$

$$a_1(x) = k^2 - \frac{4m^2}{((r_1 - r_0)x + r_1 + r_0)^2} + \mathrm{Re}(\mathcal{T}_{m,k}^2) - \frac{2\mathrm{Re}\,\mathcal{T}_{m,k}}{(r_1 - r_0)x + r_1 + r_0},$$

$$b_1(x) = \mathrm{Im}(\mathcal{T}_{m,k}^2) - \frac{2\,\mathrm{Im}\,\mathcal{T}_{m,k}}{(r_1 - r_0)x + r_1 + r_0}.$$

4.1 Mixed Fourier and Collocation Scheme

Let $\{x_j\}_{j=1}^N$ be the interior quadrature nodes in (2.1) with $\mu = 0$. The collocation approximation to (4.11) is to find $\tilde{w}_{R,m,N}(x),\ \tilde{w}_{I,m,N}(x) \in \mathbb{P}_{N+1}$ such that for $1 \le j \le N$,

$$\begin{cases} \frac{4}{(r_1-r_0)^2}\tilde{w}''_{R,m,N}(x_j) + \frac{2}{r_1-r_0}(a_0(x_j)\tilde{w}'_{R,m,N}(x_j) - b_0\tilde{w}'_{I,m,N}(x_j)) \\ \quad + a_1(x_j)\tilde{w}_{R,m,N}(x_j) - b_1(x_j)\tilde{w}_{I,m,N}(x_j) = \tilde{f}_{R,m}(x_j), \\ \frac{4}{(r_1-r_0)^2}\tilde{w}''_{I,m,N}(x_j) + \frac{2}{r_1-r_0}(b_0\tilde{w}'_{R,m,N}(x_j) + a_0(x_j)\tilde{w}'_{I,m,N}(x_j)) \\ \quad + b_1(x_j)\tilde{w}_{R,m,N}(x_j) + a_1(x_j)\tilde{w}_{I,m,N}(x_j) = \tilde{f}_{I,m}(x_j), \\ \tilde{w}_{R,m,N}(-1) = \tilde{g}_{R,m}, \qquad \tilde{w}'_{R,m,N}(1) = 0, \qquad \tilde{w}_{I,m,N}(-1) = \tilde{g}_{I,m}, \qquad \tilde{w}'_{I,m,N}(1) = 0. \end{cases} \tag{4.12}$$

Given a cut-off integer $M > 0$, the approximation to the solution of (4.5) is given by

$$w_{MN}(r,\theta) = \sum_{|m|=0}^{M} (\tilde{w}_{R,m,N}(x) + \mathrm{i}\tilde{w}_{I,m,N}(x))e^{-r\mathcal{T}_{m,k}+\mathrm{i}m\theta}, \quad \theta \in [0, 2\pi], \tag{4.13}$$

where

$$x = \frac{2}{r_1 - r_0}r - \frac{r_0 + r_1}{r_1 - r_0}.$$

Hence, it suffices to solve (4.12) for a finite number of modes m to recover the global approximation. It is straightforward to use the differentiation matrices with $\mu = 0$ in Lemma 3.1 to form the system (4.12) as in (3.4)–(3.5).

In [22], the compact combinations of Legendre polynomials, which satisfy the boundary conditions, were used for the spectral-Galerkin approximation of (4.11). It is expected that the conditioning of this approach is independent of N, but may grow like $O(k^2)$, while the conditioning of the collocation scheme (4.12) depends on k and N. However, this situation for (4.12) can be significantly relaxed by constructing a preconditioner for the resultant system as before, but it is nontrivial to design a good preconditioner for a spectral-Galerkin scheme.

4.2 Numerical Results

To check the accuracy, we take $r_0 = 1,\ r_1 = 2,\ k = 100,\ f(r,\theta) \equiv 0$ and $w_0(\theta) = e^{\sin(20\theta)}$ in (4.5). In this case, the Helmholtz equation can be solved exactly with the exact solution given by

$$w(r,\theta) = \sum_{|m|=0}^{\infty} \frac{H_m^{(1)}(kr)}{H_m^{(1)}(kr_0)}\hat{g}_m e^{\mathrm{i}m\theta},$$

where $\{\hat{g}_m\}$ are the Fourier coefficients of $w_0(\theta)$. Notice that the kernel $H_m^{(1)}(kr)/H_m^{(1)}(kr_0)$ is uniformly bounded and $|\hat{g}_m|$ decays exponentially with respect to m. Here, we truncate the infinite series and compute the modes $0 \le |m| \le 300$ as the "exact" solution. In Figs. 13 and 14, we plot the real and imaginary parts of numerical solution of (4.5) with $M = N = 170$. The corresponding discrete L^∞-errors with $M = N$ are plotted in Figs. 15 and 16, which indicates an exponential convergence rate even for large wave number k. It provides a viable alterative to the spectral-Galerkin method in [22] with an easier implementation.

Fig. 13 The numerical solution of $w(r,\theta)$: real part

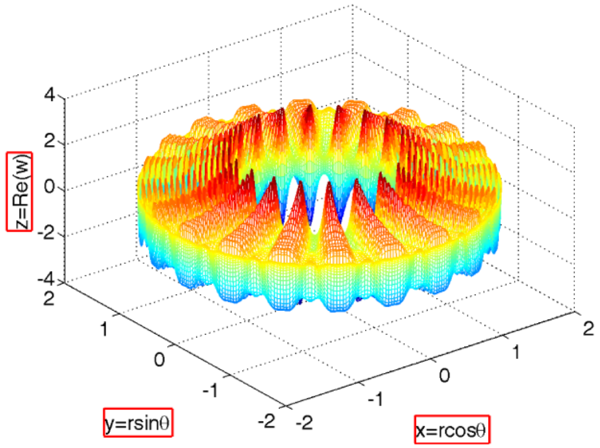

Fig. 14 The numerical solution of $w(r,\theta)$: imaginary part

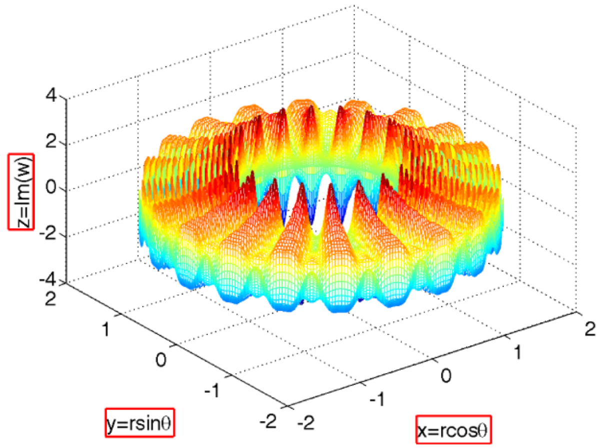

5 Concluding Remarks

We proposed in this paper a collocation method for PDEs with mixed boundary conditions based on a Gauss-Lobatto-Birkhoff type quadrature. As with the usual Gauss-Lobatto collocation methods for problems with Dirichlet data, this approach allows for an exact imposition of the underlying boundary conditions, and easy to implement. Although it is challenging to estimate the interpolation errors and analyze the collocation methods (much more involved than the analysis for the Neumann case in [26]), various numerical examples demonstrated the spectral accuracy and a convergence behavior similar to the Gauss-Lobatto collocation methods for Dirichlet problems. The idea and approach for the construction of quadrature formulas and collocation methods can be extended to propose schemes for problems with more general boundary conditions.

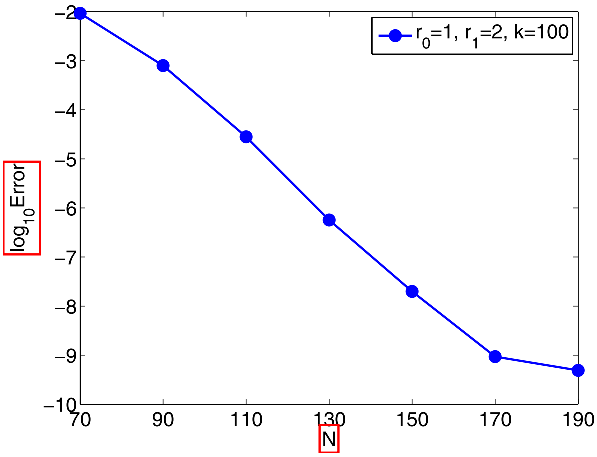

Fig. 15 L^∞-errors: real part

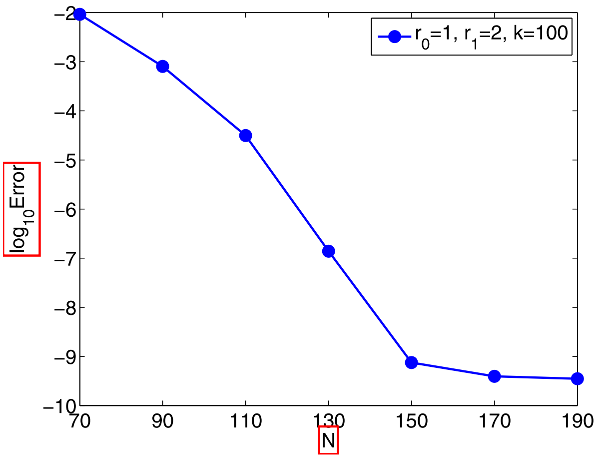

Fig. 16 L^∞-errors: imaginary part

Appendix A: Jacobi Polynomials

We recall some properties of the Jacobi polynomials (see, e.g., [24]), denoted by $J_n^{(\alpha,\beta)}(x)$, $x \in (-1,1)$ with $\alpha, \beta > -1$ and $n \geq 0$, which are mutually orthogonal with respect to the Jacobi weight $\omega^{\alpha,\beta}(x)$:

$$\int_{-1}^{1} J_n^{(\alpha,\beta)}(x) J_m^{(\alpha,\beta)}(x) \omega^{(\alpha,\beta)}(x) dx = \gamma_n^{(\alpha,\beta)} \delta_{mn}, \tag{A.1}$$

where δ_{mn} is the Knonecker symbol, and

$$\gamma_n^{(\alpha,\beta)} = \frac{2^{\alpha+\beta+1}\Gamma(n+\alpha+1)\Gamma(n+\beta+1)}{(2n+\alpha+\beta+1)\Gamma(n+1)\Gamma(n+\alpha+\beta+1)}. \tag{A.2}$$

Moreover

$$\partial_x J_n^{(\alpha,\beta)}(x) = \frac{1}{2}(n+\alpha+\beta+1) J_{n-1}^{(\alpha+1,\beta+1)}(x). \tag{A.3}$$

In this paper, we mainly use several special types of Jacobi polynomials. The first one is $J_n^{(2,1)}(x)$, defined by the three-term recursive relation

$$n(n+3)(2n+1)J_n^{(2,1)} = (n+1)(3+(2n+1)(2n+3)x)J_{n-1}^{(2,1)} - n(n+1)(2n+3)J_{n-2}^{(2,1)},$$
$$J_0^{(2,1)} = 1, \qquad J_1^{(2,1)} = \frac{5}{2}x + \frac{1}{2}, \quad x \in [-1,1]. \tag{A.4}$$

The leading coefficient of $J_n^{(2,1)}(x)$ is

$$K_n^{(2,1)} = \frac{(2n+3)!}{2^n n!(n+3)!}. \tag{A.5}$$

Moreover, we have

$$J_n^{(2,1)}(1) = \frac{(n+1)(n+2)}{2}, \qquad J_n^{(2,1)}(-1) = (-1)^n(n+1), \tag{A.6}$$

and

$$\begin{aligned} \partial_x J_n^{(2,1)}(1) &= \frac{n(n+1)(n+2)(n+4)}{12}, \\ \partial_x J_n^{(2,1)}(-1) &= \frac{(-1)^{n-1}n(n+1)(n+4)}{4}. \end{aligned} \tag{A.7}$$

The corresponding monic polynomial is defined by dividing the leading coefficient in (A.5):

$$\pi_n^{(2,1)}(x) := \lambda_n^{(2,1)} J_n^{(2,1)}(x) \quad \text{with } \lambda_n^{(2,1)} = (K_n^{(2,1)})^{-1}. \tag{A.8}$$

As a direct consequence of (A.4) and (A.8),

$$\pi_{n+1}^{(2,1)}(x) = (x-\alpha_n)\pi_n^{(2,1)}(x) - \beta_n \pi_{n-1}^{(2,1)}(x), \quad n = 0, 1, 2, \ldots, \tag{A.9}$$

where $\pi_{-1}^{(2,1)}(x) = 0, \pi_0^{(2,1)}(x) = 1$, and

$$\alpha_n = -\frac{3}{(2n+3)(2n+5)}, \qquad \beta_n = \frac{n(n+3)}{(2n+3)^2}.$$

We will also utilize the Jacobi polynomials $J_n^{(1,0)}(x)$, which are mutually orthogonal with respect to the weight $\omega^{(1,0)}(x)$. Recall that

$$J_n^{(1,0)}(1) = n+1, \qquad J_n^{(1,0)}(-1) = (-1)^n. \tag{A.10}$$

Appendix B: Formulas for the Weights of (2.1)

We first derive the expression of ω_0 as follows:

$$\begin{aligned} \omega_0 &= \frac{1}{Q_N(-1)} \int_{-1}^{1} (1+\xi_0(1+x))(\pi_N^{(2,1)}(x) + \rho\pi_{N-1}^{(2,1)}(x))dx \\ &\overset{(A.8)}{=} \frac{1}{Q_N(-1)} \int_{-1}^{1} (1+\xi_0(1+x))(\lambda_N^{(2,1)} J_N^{(2,1)}(x) + \rho\lambda_{N-1}^{(2,1)} J_{N-1}^{(2,1)}(x))dx \end{aligned}$$

$$\overset{(A.3)}{=} \frac{1}{Q_N(-1)} \int_{-1}^{1} \left(\frac{2\lambda_N^{(2,1)}}{N+3} \partial_x J_{N+1}^{(1,0)}(x) + \frac{2\rho\lambda_{N-1}^{(2,1)}}{N+2} \partial_x J_N^{(1,0)}(x) \right) dx$$

$$+ \frac{\xi_0}{Q_N(-1)} \int_{-1}^{1} (1+x)(\lambda_N^{(2,1)} J_N^{(2,1)}(x) + \rho\lambda_{N-1}^{(2,1)} J_{N-1}^{(2,1)}(x)) dx$$

$$\overset{(2.6)}{=} \frac{2}{Q_N(-1)} \left(\frac{\lambda_N^{(2,1)}}{N+3} (J_{N+1}^{(1,0)}(1) - J_{N+1}^{(1,0)}(-1)) + \frac{\rho\lambda_{N-1}^{(2,1)}}{N+2} (J_N^{(1,0)}(1) - J_N^{(1,0)}(-1)) \right)$$

$$+ \frac{4\xi_0}{Q_N(-1)} \left(\frac{N+1}{N+2} \lambda_N^{(2,1)} + \frac{N}{N+1} \rho\lambda_{N-1}^{(2,1)} \right)$$

$$\overset{(A.10)}{=} \begin{cases} \frac{2\lambda_N^{(2,1)}}{Q_N(-1)} \left(1 + \frac{2\xi_0(N+1)}{N+2}\right) + \frac{2\rho\lambda_{N-1}^{(2,1)}}{Q_N(-1)} \left(\frac{N}{N+2} + \frac{2\xi_0 N}{N+1}\right), & \text{if } N \text{ is even}, \\ \frac{2\lambda_N^{(2,1)}}{Q_N(-1)} \left(\frac{N+1}{N+3} + \frac{2\xi_0(N+1)}{N+2}\right) + \frac{2\rho\lambda_{N-1}^{(2,1)}}{Q_N(-1)} \left(1 + \frac{2\xi_0 N}{N+1}\right), & \text{if } N \text{ is odd}. \end{cases}$$

We next derive the interior weights $\{\omega_j\}_{j=1}^N$. Applying the Christoffel-Darboux formula (cf. p. 43 of Szegö [24]) to the Jacobi polynomials $\{\pi_n^{(2,1)}\}$ leads to

$$\sum_{k=0}^{N-1} \frac{\pi_k^{(2,1)}(x)\pi_k^{(2,1)}(x_j)}{(\lambda_k^{(2,1)})^2 \gamma_k^{(2,1)}} = \frac{\pi_N^{(2,1)}(x)\pi_{N-1}^{(2,1)}(x_j) - \pi_{N-1}^{(2,1)}(x)\pi_N^{(2,1)}(x_j)}{(\lambda_{N-1}^{(2,1)})^2 \gamma_{N-1}^{(2,1)}(x - x_j)}. \tag{B.1}$$

Since $Q_N(x_j) = 0$ for $1 \le j \le N$, we obtain

$$\begin{aligned} \frac{Q_N(x)}{x - x_j} &= \frac{\pi_{N-1}^{(2,1)}(x_j) Q_N(x) - \pi_{N-1}^{(2,1)}(x) Q_N(x_j)}{\pi_{N-1}^{(2,1)}(x_j)(x - x_j)} \\ &\overset{(2.2)}{=} \frac{\pi_N^{(2,1)}(x)\pi_{N-1}^{(2,1)}(x_j) - \pi_{N-1}^{(2,1)}(x)\pi_N^{(2,1)}(x_j)}{\pi_{N-1}^{(2,1)}(x_j)(x - x_j)} \\ &\overset{(B.1)}{=} \frac{(\lambda_{N-1}^{(2,1)})^2 \gamma_{N-1}^{(2,1)}}{\pi_{N-1}^{(2,1)}(x_j)} \sum_{k=0}^{N-1} \frac{\pi_k^{(2,1)}(x)\pi_k^{(2,1)}(x_j)}{(\lambda_k^{(2,1)})^2 \gamma_k^{(2,1)}}. \end{aligned}$$

Using the above formula, (2.14), (2.17), (A.8) and (2.6), we obtain that for $1 \le j \le N$,

$$\begin{aligned} \omega_j &= \int_{-1}^{1} h_j(x) dx \\ &= -\frac{\xi_j}{Q_N'(x_j)} \int_{-1}^{1} \frac{(1-x)(1+x)Q_N(x)}{x - x_j} dx \\ &\quad + \frac{\xi_j(1-x_j) + (1+x_j)^{-1}}{Q_N'(x_j)} \int_{-1}^{1} \frac{(1+x)Q_N(x)}{x - x_j} dx \\ &= \frac{(\lambda_{N-1}^{(2,1)})^2 \gamma_{N-1}^{(2,1)}}{Q_N'(x_j)\pi_{N-1}^{(2,1)}(x_j)} \left(-\xi_j \sum_{k=0}^{N-1} \frac{\pi_k^{(2,1)}(x_j)}{\lambda_k^{(2,1)} \gamma_k^{(2,1)}} \int_{-1}^{1} (1-x)(1+x) J_k^{(2,1)}(x) dx \right. \\ &\quad \left. + (\xi_j(1-x_j) + (1+x_j)^{-1}) \sum_{k=0}^{N-1} \frac{\pi_k^{(2,1)}(x_j)}{\lambda_k^{(2,1)} \gamma_k^{(2,1)}} \int_{-1}^{1} (1+x) J_k^{(2,1)}(x) dx \right) \end{aligned}$$

Table 3 The nodes and Weights of (2.1)

$\mu=1$		$\mu=0$	
Nodes	Weights	Nodes	Weights
−1.000000000000000	6.808167679121330e–2	−1.000000000000000	6.814026703724521e–2
−.7600571516720559	3.865475402538869e–1	−.7598498239875369	3.868830812252334e–1
−.2699128494272749	5.669318268665439e–1	−.2692736763599534	5.674416875675656e–1
.3134101534973076	5.681868343288488e–1	.3146082949122234	5.687958578888145e–1
.8093373187336870	4.062256170855881e–1	.8115068424004766	4.087391062811413e–1
1.000000000000000	4.026504673921036e–3	1.000000000000000	4.267941033872786e–3
−1.000000000000000	2.237899076503549e–2	−1.000000000000000	2.238108473263879e–2
−.9189661197989594	1.342468610318679e–1	−.9189585344778101	1.342594328145338e–1
−.7369294677352268	2.264787251359617e–1	−.7369048164259924	2.264999835139751e–1
−.4742346001532330	2.941125916282139e–1	−.4741852343690362	2.941403368113613e–1
−.1593664903018471	3.298759821826500e–1	−.1592872765332453	3.299074464733042e–1
.1735649466144268	3.299136070973555e–1	.1736762885919320	3.299459654404577e–1
.4885223124640942	2.942708488656596e–1	.4886656365343985	2.943024015259930e–1
.7515373707289281	2.270756377893670e–1	.7517132895385299	2.271119255381008e–1
.9356843299250334	1.411920892259339e–1	.9359403074198300	1.414514231496407e–1
1.000000000000000	4.546662779506402e–4	1.000000000000000	4.635261324086791e–4
−1.000000000000000	1.102731794921362e–2	−1.000000000000000	1.102756892230577e–2
−.9597953736228387	6.707030138488775e–2	−.9597944585074625	6.707182815450442e–2
−.8673401270440689	1.169932337314653e–1	−.8673371067847336	1.169958982777329e–1
−.7279230435919801	1.605801988037438e–1	−.7279168466735633	1.605838594198865e–1
−.5490717067631553	1.955065475007944e–1	−.5490614297002221	1.955110112814534e–1
−.3404296885411578	2.198926934901209e–1	−.3404146418749107	2.198977274979460e–1
−.1132446994806908	2.324251427396343e–1	−.1132244405475068	2.324304891910685e–1
.1202369957296858	2.324294823159141e–1	.1202626474602670	2.324348786401185e–1
.3474313656305840	2.199078899848363e–1	.3474623375760448	2.199130990872197e–1
.5560973560022953	1.955418707117604e–1	.5561333746679836	1.955467441716096e–1
.7350054455444697	1.606679604517355e–1	.7350462077554898	1.606726550298683e–1
.8745888570237517	1.172958029118844e–1	.8746348020917912	1.173022041087818e–1
.9681020629422957	7.054991921215346e–2	.9681655984928659	7.061203621749500e–2
1.000000000000000	1.116388118578149e–4	1.000000000000000	1.127078050154992e–4

$$= \frac{4(\lambda_{N-1}^{(2,1)})^2 \gamma_{N-1}^{(2,1)}}{Q_N'(x_j)\pi_{N-1}^{(2,1)}(x_j)} \Bigg(-2\xi_j \sum_{k=0}^{N-1} \frac{\pi_k^{(2,1)}(x_j)}{(k+2)(k+3)\lambda_k^{(2,1)}\gamma_k^{(2,1)}}$$
$$+ (\xi_j(1-x_j) + (1+x_j)^{-1}) \sum_{k=0}^{N-1} \frac{(k+1)\pi_k^{(2,1)}(x_j)}{(k+2)\lambda_k^{(2,1)}\gamma_k^{(2,1)}} \Bigg).$$

Finally, thanks to (2.14) and (2.17), we derive from (2.2), (A.8) and (2.6) that

$$\omega_{N+1} = \frac{4(N+1)^2\lambda_N^{(2,1)} + 4N(N+2)\rho\lambda_{N-1}^{(2,1)}}{(N+1)(N+2)(2Q_N'(1) + (2\mu+1)Q_N(1))}.$$

In Table 3, for $N = 4(4)12$, we give numerical values of the nodes and weights of (2.1) with $\mu = 1$ and 0, respectively.

References

1. Berckmann, P.: Orthogonal Polynomials for Engineers and Physicists. Golem Press, Boulder (1973)
2. Berenger, J.P.: A perfectly matched layer for the absorption of electromagnetic waves. J. Comput. Phys. **114**(2), 185–200 (1994)
3. Bernardi, C., Maday, Y.: Spectral methods. In: Ciarlet, P.G., Lions, J.L. (eds.) Techniques of Scientific Computing (Part 2). Handbook of Numerical Analysis, vol. V, pp. 209–486. Elsevier, Amsterdam (1997)
4. Boyd, J.P.: Chebyshev and Fourier Spectral Methods, 2nd edn. Dover, Mineola (2001)
5. Canuto, C.: Boundary conditions in Chebyshev and Legendre methods. SIAM J. Numer. Anal. **23**(4), 815–831 (1986)
6. Canuto, C., Hussaini, M.Y., Quarteroni, A., Zang, T.A.: Spectral Methods. Scientific Computation. Springer, Berlin (2006). Fundamentals in single domains
7. Canuto, C., Hussaini, M.Y., Quarteroni, A., Zang, T.A.: Spectral Methods. Scientific Computation. Springer, Berlin (2007). Evolution to complex geometries and applications to fluid dynamics
8. Deville, M.O., Mund, E.H.: Finite-element preconditioning for pseudospectral solutions of elliptic problems. SIAM J. Sci. Stat. Comput. **11**(2), 311–342 (1990)
9. Dyn, N., Jetter, K.: Existence of Gaussian quadrature formulas for Birkhoff type data. Arch. Math. (Basel) **52**(6), 588–594 (1989)
10. Ezzirani, A., Guessab, A.: A fast algorithm for Gaussian type quadrature formulae with mixed boundary conditions and some lumped mass spectral approximations. Math. Comput. **68**(225), 217–248 (1999)
11. Fornberg, B.: A Practical Guide to Pseudospectral Methods. Cambridge University Press, New York (1996)
12. Golub, G.H., Welsch, J.H.: Calculation of Gauss quadrature rules. Math. Comput. **23**, 221–230 (1969); Addendum, ibid., **23**(106, loose microfiche suppl) A1–A10 (1969)
13. Huang, W.Z., Sloan, D.M.: The pseudospectral method for third-order differential equations. SIAM J. Numer. Anal. **29**(6), 1626–1647 (1992)
14. Ihlenburg, F.: Finite Element Analysis of Acoustic Scattering. Applied Mathematical Sciences, vol. 132. Springer, New York (1998)
15. Jetter, K.: Uniqueness of Gauss-Birkhoff quadrature formulas. SIAM J. Numer. Anal. **24**(1), 147–154 (1987)
16. Karniadakis, G.E., Sherwin, S.J.: Spectral/*hp* Element Methods for Computational Fluid Dynamics, 2nd edn. Numerical Mathematics and Scientific Computation. Oxford University Press, New York (2005)
17. Keller, J.B., Givoli, D.: Exact non-reflecting boundary conditions. J. Comput. Phys. **82**(1), 172–192 (1989)
18. Li, J., Ma, H.P., Sun, W.W.: Error analysis for solving the Korteweg-de Vries equation by a Legendre pseudo-spectral method. Numer. Methods Partial Differ. Equ. **16**(6), 513–534 (2000)
19. Merryfield, W.J., Shizgal, B.: Properties of collocation third-derivative operators. J. Comput. Phys. **105**(1), 182–185 (1993)
20. Mulholland, L.S., Huang, W.Z., Sloan, D.M.: Pseudospectral solution of near-singular problems using numerical coordinate transformations based on adaptivity. SIAM J. Sci. Comput. **19**(4), 1261–1289 (1998)
21. Nédélec, J.C.: Acoustic and Electromagnetic Equations. Applied Mathematical Sciences, vol. 144. Springer, New York (2001). Integral representations for harmonic problems
22. Shen, J., Wang, L.L.: Analysis of a spectral-Galerkin approximation to the Helmholtz equation in exterior domains. SIAM J. Numer. Anal. **45**(5), 1954–1978 (2007) (electronic)
23. Sun, W., Huang, W., Russell, R.D.: Finite difference preconditioning for solving orthogonal collocation equations of boundary value problems. SIAM J. Numer. Anal. **33**(6), 2268–2285 (1996)
24. Szegö, G.: Orthogonal Polynomials, 4th edn., vol. 23. AMS Coll. Publ. (1975)
25. Trefethen, L.N.: Spectral methods in MATLAB. Software, Environments, and Tools. Society for Industrial and Applied Mathematics (SIAM), Philadelphia (2000)
26. Wang, L.L., Guo, B.Y.: Interpolation approximation based on Gauss-Lobatto-Legendre-Birkhoff quadrature. J. Approx. Theor. (2009). doi:10.1016/j.jat.2008.08.016
27. Wang, L.L., Guo, B.Y., Wang, Z.Q.: Generalized quadrature formula and its application to pseudospectral methods. Numer. Math. Theory Methods Appl. **11**(2), 179–196 (2002)
28. Xu, Y.: Quasi-orthogonal polynomials, quadrature, and interpolation. J. Math. Anal. Appl. **182**(3), 779–799 (1994)